Unconventional magnetoresistance induced by sperimagnetism in GdFeCo

Jaehyeon Park [1], Yuushou Hirata,[2] Jun-Ho Kang,[1] Soogil Lee [1], Sanghoon Kim,[3] Cao Van Phuoc [4], Jong-Ryul Jeong,[4]
Jungmin Park,[5] Seung-Young Park,[5] Younghun Jo [5], Arata Tsukamoto,[6] Teruo Ono,[2,7]
Se Kwon Kim,[1,*] and Kab-Jin Kim [1,†]

[1]*Department of Physics, Korea Advanced Institute of Science and Technology, Daejeon, South Korea*
[2]*Institute for Chemical Research, Kyoto University, Gokasho, Uji, Kyoto 611-0011, Japan*
[3]*Department of Physics, University of Ulsan, Ulsan 44610, South Korea*
[4]*Department of Materials Science and Engineering, Chungnam National University, Daejeon 34134, South Korea*
[5]*Center for Scientific Instrumentation, KBSI, Daejeon 34133, South Korea*
[6]*College of Science and Technology, Nihon University, Funabashi, Chiba 274-8501, Japan*
[7]*Center for Spintronics Research Network (CSRN), Graduate School of Engineering Science, Osaka University, Osaka 560-8531, Japan*

We investigate the magnetoresistance of ferrimagnetic GdFeCo across the magnetization compensation temperature T_M. The magnetic field dependence of longitudinal resistivity (ρ_{xx}) shows opposite trends below and above T_M, and the variation of ρ_{xx} with B becomes more significant as the temperature decreases. The observed unconventional magnetoresistance is attributed to the sperimagnetism of GdFeCo. Further investigations on the transverse resistivity (ρ_{xy}) of GdFeCo unveils that, contrary to the recent reports that the transition metal dominates transport of rare-earth transition-metal ferrimagnets, the Gd contribution to magnetoresistance is comparable to the FeCo contribution, showing that the transport of GdFeCo is antiferromagnetic. Our results therefore show that ferrimagnets are a convenient platform for studying antiferromagnetic spin transport and also are potential materials that can enable antiferromagnetic spin devices.

Recently, rare earth (RE)–transition metal (TM) ferrimagnetic alloys, which have been studied for magneto-optical recording traditionally [1], have been receiving a renewed interest because of the unconventional spin dynamics phenomenon which occurs at the magnetization compensation temperature T_M or the angular momentum compensation temperature T_A. Recent experiments have shown that a fast domain-wall motion can be achieved near the T_A of ferrimagnets due to the emergence of pure antiferromagnetic spin dynamics at T_A [2–4]. The disappearance of the skyrmion Hall effect, which was expected in antiferromagnets, has also been reported at T_A of ferrimagnets [5,6]. Besides the magnetization dynamics, a highly efficient spin-orbit torque or spin-transfer torque have been reported near the T_M or the T_A [7–10], which makes ferrimagnets more promising candidates for spintronic applications.

Contrary to the newly discovered spin dynamics phenomena, the transports of RE-TM ferrimagnets have not been updated for a long time. Despite the intensive studies on the transport properties of ferrimagnets that were done several decades ago [11–19,22–24], there remains a significant number of open questions on their transport mechanisms. In particular, it is a long-standing issue whether the transport of RE-TM ferrimagnets is associated with solely either the RE submoment [11,12] or the TM submoment [13–18], or

with both submoments [19]. The early studies assigned a dominant role to either one of two submoments [11–18] or both submoments [19], but most recent works have assumed that the TM plays a dominant role in the transport of ferrimagnets [2,7,20,21]. However, there has been no universally accepted consensus on this issue, mainly because of the lack of an experimental scheme to identify the transport of RE-TM ferrimagnets.

In this work, we tackle this long-standing problem by exploring longitudinal and transverse resistivities of GdFeCo. The longitudinal resistivity ρ_{xx}, which reflects the change of anisotropic magnetoresistance (AMR), is found to depend on the magnetic field B and temperature T in a distinct way: the ρ_{xx} increases with increasing B for $T < T_M$, while it decreases for $T > T_M$, and the slope of $\rho_{xx}-B$ curve increases as the temperature decreases. On the other hand, the transverse resistivity ρ_{xy}, which exhibits conventional anomalous Hall effect (AHE), has little dependence on the external magnetic field. The observed field and temperature dependence of the magnetoresistance of GdFeCo qualitatively differs from those of ferromagnetic transition metals.

These unconventional longitudinal and transverse magnetoresistances can be explained by the antiferromagnetic nature of the magnetic coupling and the ensuing sperimagnetism of GdFeCo. Fe and Gd moments in GdFeCo are coupled antiferromagnetically but their directions are spatially dispersed due to the weak exchange interactions [22–24] [Fig. 1(a)]. When a magnetic field is applied to sperimagnetic GdFeCo, the cone angle of each submoment either increases or decreases
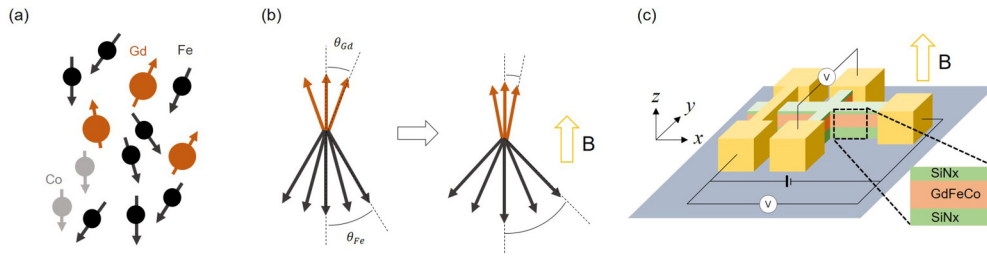
FIG. 1. (a) The distribution of the magnetic moments in an amorphous GdFeCo alloy. The brown arrows represent the Gd magnetic moments. The black and gray arrows denote the Fe and the Co respectively. (b) Schematic illustration of the sperimagnetic GdFeCo. The Gd and Fe moments are distributed with cone angles of θ_{Gd} and θ_{Fe}. (c) Schematic of the GdFeCo device with measurement geometry.

depending on the relative direction between the submagnetic moment and the external field [Fig. 1(b)]. This field-induced opposite change of the two cone angles can explain the observed magnetoresistances as we will detail below. Our results suggest that the unconventional resistance change of GdFeCo is, contrary to the recent reports [2,7,20,21], caused by both the RE and the TM submoments.

For this study, we prepared two 30-nm-thick GdFeCo films deposited on a Si_3N_4 substrate by magnetron sputtering. Two films have a slightly different composition: $Gd_{23.5}Fe_{66.9}Co_{9.6}$ for sample 1 and $Gd_{23}Fe_{67.4}Co_{9.6}$ for sample 2. In the following, we focus on sample 1, but we have confirmed that the overall results of sample 2 are the same as those of sample 1. 5 nm of the Si_3N_4 layer was capped at the top of the film to prevent oxidization. The GdFeCo films have a perpendicular magnetic anisotropy (PMA), in which Gd and FeCo are coupled antiferromagnetically. The microscopic structure of GdFeCo has been reported in other works [25,26], where the typical size of grain was confirmed to be on the order of a few nanometers. We note that Fe concentration is much larger than Co in TM, so that the GdFeCo is more similar to the GdFe rather than the GdCo [22]. The film was then patterned into a microwire with Hall bar by electron beam lithography and Ar ion milling. The length and width of the microwire are 40 and 10 μm, respectively. Ti (5 nm)/Au (100 nm) was used as the electrode to measure the transport. A current of 1 mA (of which current density is 3.3×10^9 A/m^2) was injected along the x direction and the longitudinal (V_{xx}) and transverse voltage (V_{xy}) were measured to determine ρ_{xx} and ρ_{xy}. The schematic illustration of our device and measurement geometry are shown in Fig. 1(c).

We first measure the transverse resistance of GdFeCo by sweeping a magnetic field at various temperatures. The magnetic field is applied along the out-of-plane direction [z direction in Fig. 1(c)] up to 2 T. Here we limit the maximum magnetic field by 2 T because the GdFeCo shows spin-flop transition above this field [27]. As shown in Fig. 2(a), the transverse resistance exhibits a hysteresis loop which corresponds to the AHE of GdFeCo. A clear square shape of the loop indicates the PMA of patterned GdFeCo. The reversal of the loop polarity as well as the large enhancement of coercive field (B_c) is observed between 150 and 170 K, suggesting that the T_M exists between these temperatures [2,19]. Since the loop polarity changes from positive to negative as we decrease the temperature, we can determine the dominant submagnetic moment at each temperature region [19]: FeCo is dominant (with respect to the magnetization) for $T > T_M$, while Gd is

dominant for $T < T_M$. Figure 2(b) shows the anomalous Hall resistivity, $\rho_H = (\rho_{xy}^{up} + \rho_{xy}^{down})/2$, extracted from Fig. 2(a). Here, ρ_{xy}^{up} is the transverse resistivity of a remnant state after applying $B = 2$ T, while ρ_{xy}^{down} is the transverse resistivity of a remnant state after applying $B = -2$ T. The black and orange symbols correspond to the FeCo–moment-dominant and the Gd–moment-dominant temperature regions, respectively, and the open symbols represent the sign reversal of Hall resistivity. The magnitude of the Hall resistivity slightly increases as the temperature decreases, which may be due to the effect of the variation of the longitudinal resistivity at low temperatures. The value is about $|\rho_H| = 11-13$ $\mu\Omega$ cm which is consistent with previous reports for GdFe alloys [28,29].

We next investigate the longitudinal resistivity ρ_{xx} of GdFeCo. Figure 3(a) shows the resistivity variation as a function of temperature. The ρ_{xx} increases monotonically as the temperature decreases, which may be due to the amorphous nature of our GdFeCo sample where strong disorders localize the electrons at low temperatures [28]. The value is about 235–245 $\mu\Omega$ cm which is consistent with the previous reports for GdFe [28,29]. We note that the slight temperature variation of ρ_{xx} does not affect the unconventional MR which we discuss later. Figure 3(b) shows the field-dependent resistivity variation, $\Delta\rho_{xx}(B)/\rho_{xx}(B=0)$, for various temperatures. The resistivity is found to either increase or decrease with the magnetic field, and forms a bowtie shape. We attribute the observed variation of the longitudinal resistivity to the combined effect of AMR and sperimagnetic nature of GdFeCo as follows. As stated above, GdFeCo is known as a sperimagnet [22], because the directions of Fe moments are randomly distributed and form a cone angle due to the weak Fe-Fe exchange interaction. Furthermore, since the Gd-Fe antiferromagnetic exchange interaction is much stronger than the Gd-Gd ferromagnetic exchange interaction [23,24], Gd moments are likely to be dispersed and form a cone angle, as shown in Figs. 1(a) and 1(b). According to Ref. [22], the GdFeCo exhibits sperimagnetism when the composition ratio of the Co is less than 30%, which is the case in our GdFeCo (9.6% of Co). Therefore, our GdFeCo can be considered as a sperimagnet whose Gd and Fe moments form cone angles θ_{Gd} and θ_{Fe}, respectively [Fig. 1(b)].

The sperimagnetic nature of GdFeCo can explain the observed field-dependent resistivity variation. Figure 3(c) shows the representative resistivity variation at $T = 100$ K with schematic illustration of two submoments. Since the temperature is lower than the magnetization compensation temperature ($T_M = 150-170$ K), the Gd submoment
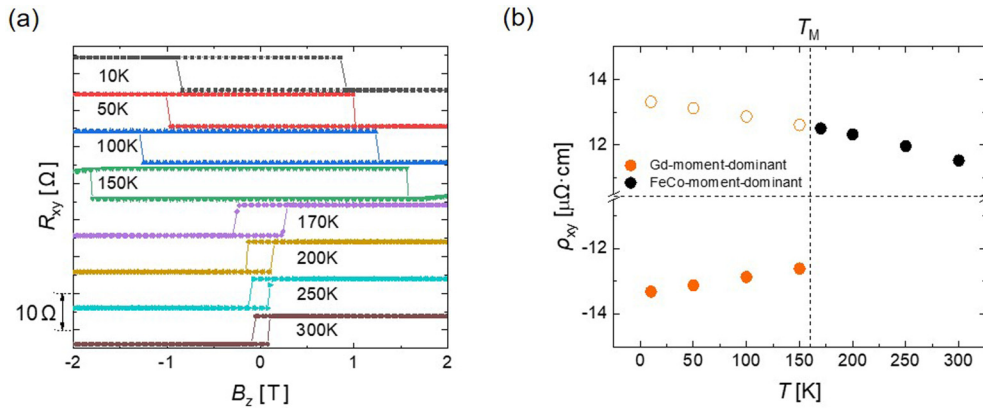
FIG. 2. (a) The Hall resistance R_{xy} as a function of magnetic field measured from 10 to 300 K. Different colors correspond to the different temperatures as denoted in the figure. (b) The anomalous Hall resistivity $\rho_H = (\rho_{xy}^{up} + \rho_{xy}^{down})/2$ extracted from (a). The black symbols represent the ρ_H for $T > T_M$ and the orange symbols represent the ρ_H for $T < T_M$. The open symbols denote the opposite sign of ρ_H.

dominates over the Fe submoment. If we apply $+2$ T along the $+z$ direction, then the Gd moments are directed to the $+z$ direction whereas the FeCo moments are aligned to the $-z$ direction, since they are antiferromagnetically coupled to each other. At $B_Z = +2$ T, the Gd (Fe) moments are parallel (antiparallel) to the magnetic field, so their cone angles are small (large) because the Zeeman interaction suppresses (expands) the cone angle. When the strength of magnetic field is reduced to zero, the cone angle of Gd (Fe) increases (decreases) due to the release of the Zeeman energy. When we further sweep the magnetic field to the negative value, the cone angle of Gd (Fe) further increases (decreases) up to the coercive field, because the Gd (Fe) moments are antiparallel (parallel) to the magnetic field. At the coercive field, the Gd (Fe) moments are abruptly switched to the $-z$ ($+z$) direction and becomes parallel (antiparallel) to the magnetic field. After the switching, the Gd (Fe) moments are maintained parallel (antiparallel) to the magnetic field, which reduces (increases) the cone angle. When we further increase the magnetic field to the negative value, then the cone angle of Gd (Fe) moments decreases (increases) due to the Zeeman interaction. A similar sequence is repeated for the field sweep from negative to positive field. Since the AMR depends on the cone angle of each submoment, as we will discuss later with more a detailed

model, the bowtie shape of the resistance can be obtained for the field sweep experiment.

We note that the field-dependent resistivity variation is similar with the magnon magnetoresistance (MMR) observed in 3 d transition metals [30–32]. However, this possibility can be excluded for the following reason. In Fig. 4(a), we select data from $B_Z = +2$ T to $B_Z = 0$ T from Fig. 3(b), where the dominant submoment is aligned along the magnetic field direction. It is clear that the ρ_{xx} increases with B for $T < T_M$, while it decreases with B for $T > T_M$. The slopes of $\rho_{xx}-B$ in Fig. 4(a) are summarized in Fig. 4(b). The slope increases with decreasing temperature with a sign reversal at T_M. This result is in opposition to what is expected for MMR, where the field-induced resistivity variation comes from thermal magnon excitations and thus should be suppressed at low temperatures [30,32]. Therefore, the observed resistivity variation cannot be explained in the frame of the magnon-mediated model.

We model AMR ($\rho_{AMR} = \rho^{\parallel} - \rho^{\perp}$) of GdFeCo by $\rho_{AMR} = A\langle(m_x^{Fe})^2\rangle + B\langle(m_x^{Gd})^2\rangle$, where $\rho^{\parallel}$ ($\rho^{\perp}$) is the resistivities when the average magnetization and current are parallel (perpendicular), A and B represent the magnitude and the sign of AMR of Fe and Gd, respectively, x is the direction of the current, m_x^{Fe} (m_x^{Gd}) is the x component
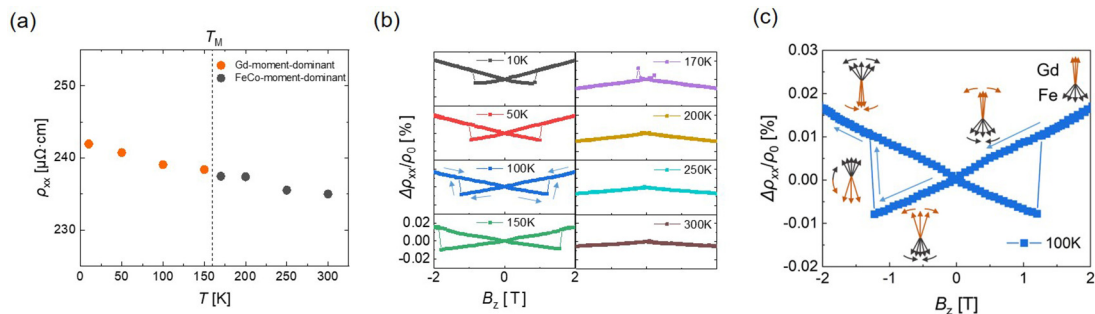

FIG. 3. (a) The resistivity ρ_{xx} measured at various temperatures without external field. The black symbols represent the ρ_{xx} for $T > T_M$ and the orange symbols represent the ρ_{xx} for $T < T_M$. (b) The variation of ρ_{xx} as a function of magnetic field for various temperature. Different colors correspond to the different temperatures as denoted in the figure. (c) The extracted result for $T = 100$ K with schematic illustrations of two submoments.
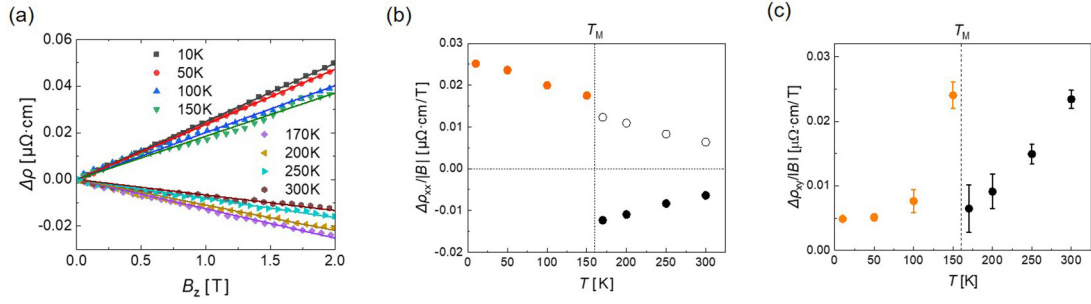
FIG. 4. (a) The extracted field-dependent resistivity variation for $B_Z = +2$ T to 0 T from Fig. 3(b). (b) The slope of $\rho_{xx} - B$ extracted from (a). The black symbols represent the slope $\Delta\rho_{xx}/B$ for $T > T_M$ and the orange symbols represent the $\Delta\rho_{xx}/B$ for $T < T_M$. Open symbols denote the opposite sign of $\Delta\rho_{xx}/B$. (c) The slope of $\rho_{xy} - B$ extracted from Fig. 2(a). The black symbols represent the slope $\Delta\rho_{xy}/B$ for $T > T_M$ and the orange symbols represent the $\Delta\rho_{xy}/B$ for $T < T_M$.

of the magnetization unit vector of the random Fe (Gd) site, and $\langle X \rangle$ is the average of the random value X. According to Fig. 2 of Ref. [33], the Fe has positive AMR, that is $A > 0$. On the other hand, the Gd has negative AMR, that is $B < 0$, as shown in Fig. 1 of Ref. [34]. Here we treat the contributions of Fe and Gd independently, because the mean free path of amorphous Gd alloys (which is a few Å [35]) is much smaller than the typical grain size of Gd and Fe in GdFeCo (which is a few tens of Å [25,26]). We assume that $\langle (m_x^{Fe})^2 \rangle = \langle (m_y^{Fe})^2 \rangle = (1 - \langle (m_z^{Fe})^2 \rangle)/2 = (\sin^2\theta_{Fe})/2$ and the same for Gd by assuming isotropy in spin xy space. Then, we have

$$\rho_{AMR} = \frac{A+B}{2} - \frac{A\langle (m_z^{Fe})^2 \rangle + B\langle (m_z^{Gd})^2 \rangle}{2}. \quad (1)$$

Equation (1) indicates that the contributions from Fe and Gd to AMR add up destructively because $A > 0$ and $B < 0$ [33,34] and thereby result in a small value of AMR of GdFeCo compared to that of $3d$ transition metals [21]. Next, we obtain the variation of AMR by out-of-plane magnetic field,

$$\frac{\partial \rho_{AMR}}{\partial B_z} \approx -A\langle m_z^{Fe} \rangle \left\langle \frac{\partial m_z^{Fe}}{\partial B_z} \right\rangle - B\langle m_z^{Gd} \rangle \left\langle \frac{\partial m_z^{Gd}}{\partial B_z} \right\rangle, \quad (2)$$

where the approximation is taken by assuming a small covariance of m_z^{Fe} and $\frac{\partial m_z^{Fe}}{\partial B_z}$. Then, for $T > T_M$, where the Fe (Gd) submoment is parallel (antiparallel) to the B_z, $m_z^{Fe} > 0$ and $m_z^{Gd} < 0$. Since $\frac{\partial m_z^{Fe}}{\partial B_z} > 0$ and $\frac{\partial m_z^{Gd}}{\partial B_z} > 0$ at any temperature, we obtain $A\langle m_z^{Fe} \frac{\partial m_z^{Fe}}{\partial B_z} \rangle > 0$ and $B\langle m_z^{Gd} \frac{\partial m_z^{Gd}}{\partial B_z} \rangle > 0$ and thus $\frac{\partial \rho_{AMR}}{\partial B_z} < 0$, explaining the negative slope of the $\rho_{xx} - B$ curve for $T > T_M$ [see Fig. 4(a)]. Note that the contributions from Fe and Gd to $\frac{\partial \rho_{AMR}}{\partial B_z}$ add up constructively, because they have the same sign. For $T < T_M$, on the other hand, the Gd (Fe) submoment is parallel (antiparallel) to the B_z. Thus, we have $m_z^{Fe} < 0$ and $m_z^{Gd} > 0$. Considering that $\frac{\partial m_z^{Fe}}{\partial B_z} > 0$ and $\frac{\partial m_z^{Gd}}{\partial B_z} > 0$, we obtain $A\langle m_z^{Fe} \frac{\partial m_z^{Fe}}{\partial B_z} \rangle < 0$ and $B\langle m_z^{Gd} \frac{\partial m_z^{Gd}}{\partial B_z} \rangle < 0$ and thus $\frac{\partial \rho_{AMR}}{\partial B_z} > 0$, confirming the positive slope of the $\rho_{xx} - B$ curve for $T < T_M$ [see Fig. 4(a)]. The contributions from Fe and Gd to $\frac{\partial \rho_{AMR}}{\partial B_z}$ add up constructively again. Therefore, the simple analysis based on Eqs. (1) and (2) well explains the qualitative features of the observed $\rho_{xx} - B$ curve for all temperatures. Two remarks

are in order. First, our model can explain the larger value of ρ_{xx}/B at low temperatures [Fig. 4(b)], because the AMR of GdFeCo increases at low temperatures [21]. Second, the contributions from Fe and Gd are destructive to ρ_{AMR}, while they are constructive to $\frac{\partial \rho_{AMR}}{\partial B_z}$. This explains a large variation in the $\rho_{xx} - B$ curve despite the small AMR of GdFeCo. In fact, the AMR of GdFeCo is as small as 0.1% at 10 K [21], but the AMR variation by magnetic field of 2 T is about 0.02% which is 20% of the total AMR.

The situation is quite different for the transverse resistivity. The AHE can be modeled by [36]

$$\rho_{AHE} = C\langle M_z^{Fe} \rangle + D\langle M_z^{Gd} \rangle, \quad (3)$$

where $C > 0$ and $D < 0$ represent the magnitude and the sign of AHE of Fe and Gd, respectively [19,29,36], and M_z^{Fe} (M_z^{Gd}) is the magnetization of the Fe (Gd) sublattice. Equation (3) indicates that the contributions from Fe and Gd to AHE add up constructively because M_z^{Fe} and M_z^{Gd} are always directed opposite in ferrimagnets and $C > 0$ and $D < 0$ [19,29,36]. This results in a large value of AHE in GdFeCo [19]. Next, we obtain the variation of AHE by out-of-plane magnetic field,

$$\frac{\partial \rho_{AHE}}{\partial B_z} = C\left\langle \frac{\partial M_z^{Fe}}{\partial B_z} \right\rangle + D\left\langle \frac{\partial M_z^{Gd}}{\partial B_z} \right\rangle. \quad (4)$$

Since $\frac{\partial M_z^{Fe}}{\partial B_z} > 0$ and $\frac{\partial M_z^{Gd}}{\partial B_z} > 0$ at any temperatures, $C\langle \frac{\partial M_z^{Fe}}{\partial B_z} \rangle > 0$ and $D\langle \frac{\partial M_z^{Gd}}{\partial B_z} \rangle < 0$. Therefore, the contributions from Fe and Gd to $\frac{\partial \rho_{AHE}}{\partial B_z}$ add up destructively. This implies that variation of ρ_{xy} of GdFeCo by a magnetic field can be small, although ρ_{xy} itself is large. In Fig. 4(c) we plot the slope of $\rho_{xy} - B$ curve extracted from Fig. 2(a). The result shows that the variation of ρ_{xy} by magnetic field is merely 0.1–0.3% of the total AHE, which is indeed very small.

Most recent works have assumed that the transport of RE-TM ferrimagnet is dominated by the TM submoment [2,7,8,20,21]. Let us assume that this is the case: the observed resistivity variations in Figs. 4(b) and 4(c) induced by the external field are caused by the field-induced change of the TM cone angle θ_{Fe} only. Since $\rho_{AMR} \propto \langle (m_x^{Fe})^2 \rangle = \sin^2\theta_{Fe}$ and $\rho_{AHE} \propto \cos\theta_{Fe}$, we have, for small field-induced changes of the Fe cone angle $\Delta\theta_{Fe}$, $\frac{\Delta\rho_{AMR}}{\rho_{AMR}} = (2\cot\theta_{Fe})\Delta\theta_{Fe}$ and $\frac{\Delta\rho_{AHE}}{\rho_{AHE}} = (\tan\theta_{Fe})\Delta\theta_{Fe}$. Note that we observed the large

variation of ρ_{xx} (20% of AMR) and the small variation of ρ_{xy} (0.1–0.3% of AHE) by the application of the external field of 2 T, and thus $(\frac{\Delta\rho_{AMR}}{\rho_{AMR}})/(\frac{\Delta\rho_{AHE}}{\rho_{AHE}}) \sim 100$. This experimental observation and the aforementioned simple TM-only analysis leads us to conclude that $\theta_{Fe} \sim 0$ with no dispersion of magnetic moments, but this is contradictory to the existing results on sperimagnetism of GdFeCo [22–24]. Instead, as we discussed, the observed resistivity variation can be well explained by taking into account the contributions from both θ_{Fe} and θ_{Gd} change. Therefore, the resistivity variations induced by sperimagnetism suggest that, contrary to the recent reports [2,7,8,20,21], both the RE and the TM submoments participate in the transport of RE-TM ferrimagnets and thus antiferromagnetic transport, where conduction electrons interact with two or multiple antiferromagnetically coupled submoments, takes place in RE-TM ferrimagnets. Our result indicates that RE-TM ferrimagnets can serve as versatile platform to study nonequilibrium antiferromagnetic transport properties such as antiferromagnetic spin-transfer torque and also the spin polarization compensation point with zero spin polarization of conduction electrons. Further research might enable us to achieve the pure antiferromagnetic transport by tuning the relative composition of RE and TM.

In summary, we investigated the transport properties of ferrimagnetic GdFeCo across the magnetization compensation temperature. The longitudinal resistivity was found to increase with magnetic field for $T < T_M$, while it decreased for $T > T_M$. The transverse resistivity, on the other hand, had little dependence on magnetic field. We attribute the unconventional resistivity variation to the combined effect of anisotropic magnetoresistance and sperimagnetic nature of GdFeCo. Based on the simple analysis, in which the contributions from Gd and Fe to the resistivities are assumed to be independent, we found that the Gd and Fe submoments contribute to longitudinal resistivity constructively, while they contribute to transverse resistivity destructively. Our results therefore suggest that the resistance change of GdFeCo occurs through both the RE and the TM submoments, invalidating the conventional wisdom that its transport properties are dominantly governed by one of several constituent elements.

[1] A. Kirilyuk, A. V. Kimel, and T. Rasing, Rev. Mod. Phys. **82**, 2731 (2010).

[2] K. J. Kim, S. K. Kim, Y. Hirata, S. H. Oh, T. Tono, D. H. Kim, T. Okuno, W. S. Ham, S. Kim, G. Go, Y. Tserkovnyak, A. Tsukamoto, T. Moriyama, K. J. Lee, and T. Ono, Nat. Mater. **16**, 1187 (2017).

[3] S. A. Siddiqui, J. Han, J. T. Finley, C. A. Ross, and L. Liu, Phys. Rev. Lett. **121**, 057701 (2018).

[4] L. Caretta, M. Mann, F. Büttner, K. Ueda, B. Pfau, C. M. Günther, P. Hessing, A. Churikova, C. Klose, M. Schneider, D. Engel, C. Marcus, D. Bono, K. Bagschik, S. Eisebitt, and G. S. D. Beach, Nat. Nanotechnol. **13**, 1154 (2018).

[5] Y. Hirata, D. H. Kim, S. K. Kim, D. K. Lee, S. H. Oh, D. Y. Kim, T. Nishimura, T. Okuno, Y. Futakawa, H. Yoshikawa, A. Tsukamoto, Y. Tserkovnyak, Y. Shiota, T. Moriyama, S. B. Choe, K. J. Lee, and T. Ono, Nat. Nanotechnol. **14**, 232 (2019).

[6] S. Woo, K. M. Song, X. Zhang, Y. Zhou, M. Ezawa, X. Liu, S. Finizio, J. Raabe, N. J. Lee, S. Il Kim, S. Y. Park, Y. Kim, J. Y. Kim, D. Lee, O. Lee, J. W. Choi, B. C. Min, H. C. Koo, and J. Chang, Nat. Commun. **9**, 959 (2018).

[7] R. Mishra, J. Yu, X. Qiu, M. Motapothula, T. Venkatesan, and H. Yang, Phys. Rev. Lett. **118**, 167201 (2017).

[8] R. Blasing, T. Ma, S.-H. Yang, C. Garg, F. K. Dejene, A. T. N'Diaye, G. Chen, and S. S. P. Parkin, Nat. Commun. **9**, 4984 (2018).

[9] S. G. Je, J. C. Rojas-Sánchez, T. H. Pham, P. Vallobra, G. Malinowski, D. Lacour, T. Fache, M. C. Cyrille, D. Y. Kim, S. B. Choe, M. Belmeguenai, M. Hehn, S. Mangin, G. Gaudin, and O. Boulle, Appl. Phys. Lett. **112**, 062401 (2018).

[10] T. Okuno, D. H. Kim, S. H. Oh, S. K. Kim, Y. Hirata, T. Nishimura, W. S. Ham, Y. Futakawa, H. Yoshikawa, A. Tsukamoto, Y. Tserkovnyak, Y. Shiota, T. Moriyama, K. J. Kim, K. J. Lee, and T. Ono, Nat. Electron. **2**, 389 (2019).

[11] A. Ogawa, T. Katayama, M. Hirano, and T. Tsushima, in *Magnetism and Magnetic Materials-1974: 20th Annual Conference, San Francisco*, edited by C. D. Graham, Jr., G. H. Lander, and J. J. Rhyne, AIP Conf. Proc. No. 24 (AIP, New York, 1975), p. 575.

[12] A. Ogawa, T. Katayama, M. Hirano, and T. Tsushima, Jpn. J. Appl. Phys. **15**, 87 (1976).

[13] R. Hasegawa, B. E. Argyle, and L.-J. Tao, in *Magnetism and Magnetic Materials-1974: 20th Annual Conference, San Francisco* (Ref. [11]), p. 110.

[14] B. E. Argyle, R. J. Gambino, and K. Y. Ahn, in *Magnetism and Magnetic Materials-1974: 20th Annual Conference, San Francisco* (Ref. [11]), p. 564.

[15] T. Shirakawa, Y. Nakajima, K. Okamoto, S. Matsushita, and Y. Sakurai, in *Magnetism and Magnetic Materials – 1976: Proceedings of the First Joint MMM-Intermag Conference*, edited by H. C. Wolfe, J. J. Becker, and G. H. Lander, AIP Conf. Proc. No. 34 (AIP, New York, 1976), p. 349.

[16] Y. Mimura, N. Imamura, and Y. Kushiro, J. Appl. Phys. **47**, 3371 (1976).

[17] R. Asomoza, I. A. Campbell, H. Jouve, and R. Meyer, J. Appl. Phys. **48**, 3829 (1977).

[18] R. Malmhäll, J. Appl. Phys. **54**, 5128 (1983).

[19] T. R. McGuire, R. J. Gambino, and R. C. Taylor, J. Appl. Phys. **48**, 2965 (1977).

[20] J. Finley and L. Liu, Phys. Rev. Appl. **6**, 054001 (2016).

[21] T. Okuno, K. J. Kim, T. Tono, S. Kim, T. Moriyama, H. Yoshikawa, A. Tsukamoto, and T. Ono, Appl. Phys. Express **9**, 073001 (2016).

[22] R. C. Taylor and A. Gangulee, Phys. Rev. B **22**, 1320 (1980).

[23] M. Mansuripur and M. F. Ruane, IEEE Trans. Magn. **MAG-22**, 33 (1986).

[24] P. Hansen, C. Clausen, G. Much, M. Rosenkranz, and K. Witter, J. Appl. Phys. **66**, 756 (1989).

[25] C. E. Graves, A. H. Reid, T. Wang, B. Wu, S. De Jong, K. Vahaplar, I. Radu, D. P. Bernstein, M. Messerschmidt, L. Müller, R. Coffee, M. Bionta, S. W. Epp, R. Hartmann, N. Kimmel, G. Hauser, A. Hartmann, P. Holl, H. Gorke, J. H. Mentink *et al.*, Nat. Mater. **12**, 293 (2013).

[26] C. Kim, S. Lee, H.-G. Kim, J.-H. Park, K.-W. Moon, J. Y. Park, J. M. Yuk, K.-J. Lee, B.-G. Park, S. K. Kim, K.-J. Kim, and C. Hwang, Nat. Mater. **19**, 980 (2020).

[27] J. Becker, A. Tsukamoto, A. Kirilyuk, J. C. Maan, T. Rasing, P. C. M. Christianen, and A. V. Kimel, Phys. Rev. Lett. **118**, 117203 (2017).

[28] T. R. McGuire, R. C. Taylor, and R. J. Gambino, in *Magnetism and Magnetic Materials – 1976: Proceedings of the First Joint MMM-Intermag Conference* (Ref. [15]), p. 346.

[29] T. R. McGuire, R. J. Gambino, and R. C. Taylor, IEEE Trans. Magn. **13**, 1598 (1977).

[30] B. Raquet, M. Viret, E. Sondergard, O. Cespedes, and R. Mamy, Phys. Rev. B **66**, 024433 (2002).

[31] A. P. Mihai, J. P. Attané, A. Marty, P. Warin, and Y. Samson, Phys. Rev. B **77**, 060401(R) (2008).

[32] V. D. Nguyen, L. Vila, P. Laczkowski, A. Marty, T. Faivre, and J. P. Attané, Phys. Rev. Lett. **107**, 136605 (2011).

[33] T. R. Mcguire and R. I. Potter, IEEE Trans. Magn. **11**, 1018 (1975).

[34] K. A. McEwen, G. D. Webber, and L. W. Roeland, Physica B+C **86-88**, 533 (1977).

[35] T. Kaneyoshi, *Amorphous Magnetism* (CRC, Boca Raton, 1984).

[36] W. J. Xu, B. Zhang, Z. X. Liu, Z. Wang, W. Li, Z. B. Wu, R. H. Yu, and X. X. Zhang, Europhys. Lett. **90**, 27004 (2010).